

A Coupled Model of the Global Cycles of Carbonyl Sulfide and CO₂: A Possible New Window on the Carbon Cycle

Joe Berry^{1*}, Ian Baker², Elliott Campbell³, S. Randy Kawa⁴, A. Scott Denning², Zhengxin Zhu⁴, Stephen Montzka⁵, Adam Wolf⁶, Ulrike Seibt⁷

1. Carnegie Institution, Dept. of Global Ecology, Stanford, CA
2. Dept. Atmos. Sci. Colorado State Univ. Ft. Collins, CO
3. Sierra Nevada Research Institute, University of California, Merced CA
4. NASA, GSFC, Greenbelt, MD
5. NOAA-ESRL, Boulder, CO
6. Dept. of Ecology & Evolutionary Biology, Princeton University, Princeton NJ
7. Dept of Atmospheric and Oceanic Sciences, University of California, Los Angeles CA

* Corresponding author: joeberry@stanford.edu

Running title: Carbonyl sulfide as global carbon cycle tracer

1 **Abstract**

2 Carbonyl sulfide (COS) is an atmospheric trace gas that participates in some key reactions
3 of the carbon cycle, and thus holds great promise for studies of carbon cycle processes.
4 Global monitoring networks and atmospheric sampling programs provide concurrent data
5 on COS and CO₂ concentration in the free troposphere and atmospheric boundary layer
6 over vegetated areas. Here, we present a modeling framework for interpreting these data,
7 and illustrate what COS measurements might tell us about carbon cycle processes. We
8 implemented mechanistic and empirical descriptions of leaf and soil COS uptake into a
9 global carbon cycle model (SiB 3), and obtained new COS flux estimates based on
10 environmental conditions and physiological stress. We then used an atmospheric transport
11 model (PCTM) to simulate the variations in the concentration of COS and CO₂ in the global
12 atmosphere. To balance the 3-fold increase in the global vegetation sink, we propose a
13 revision of the global ocean COS source. The new model is capable of reproducing the
14 seasonal variation in atmospheric concentration at most background atmospheric sites.
15 The model also reproduces the observed large vertical gradients in COS between the
16 boundary layer and free troposphere. Using a simulation experiment, we demonstrate that
17 comparing drawdown of CO₂ with COS could provide additional constraints on differential
18 responses of photosynthesis and respiration to environmental forcing. The separation of
19 these two distinct processes is essential to understand the carbon cycle components for
20 improved prediction of future responses of the terrestrial biosphere to changing
21 environmental conditions.

22 **Introduction**

23 Carbonyl sulfide (COS) is an atmospheric trace gas that holds great promise for studies of
24 carbon cycle processes (Montzka et al. 2007, Campbell et al. 2008, Suntharalingam et al.
25 2008, Blonquist et al. 2011, Wohlfahrt et al. 2012). COS is an analog of CO₂. It participates
26 in some key reactions of the carbon cycle, and monitoring its concentration, like that of the
27 ¹³C and ¹⁸O isotopologues of CO₂, provides additional information on carbon cycle
28 processes. Specifically, COS is taken up by reactions associated with leaf photosynthesis
29 and microbial activity in soils. Unlike for CO₂, soils are generally a sink for COS (Van Diest
30 and Kesselmeier 2008). The drawdown of COS concentration over the continents is,
31 therefore, related to the sum of photosynthesis and soil microbial activity, while that of CO₂
32 is related to the difference between leaf photosynthesis and soil respiration. The main
33 source of COS is biogenic activity in the ocean (Cutter et al. 2004), and uptake by leaves and
34 soil are its main sink. Atmospheric chemistry and anthropogenic sources, while significant
35 in the global budget, play only a minor role in driving changes in COS concentration over
36 most vegetated regions in the absence of fires (Montzka et al. 2007, Campbell et al. 2008).
37 The NOAA-ESRL global monitoring network provides a multiannual record of COS at 14
38 background atmospheric sampling sites. This atmospheric sampling programs has
39 collected approximately eight thousand point measurements of COS and CO₂ concentration
40 from tower sites and aircraft in the free troposphere and atmospheric boundary layer over
41 vegetated areas per year (Montzka et al. 2007). Some measurements of COS concentration
42 are now being obtained from the ACE satellite (Barkley et al. 2008), and there are
43 prospects for expanded sampling of this trace gas from satellite and surface locations. The

44 goal of the present study is to develop a modeling framework for interpreting these data,
45 and to illustrate what COS measurements might tell us about carbon cycle processes.

46 **Methods**

47 **Transport Models**

48 We chose to use the Parameterized Chemical Transport Model (PCTM)¹ and
49 meteorology from NASA's GEOS-4 model² to simulate the 3-D variation in the
50 concentration of CO₂ and COS in the global atmosphere given gridded fields of the surface
51 sources and sinks of COS and CO₂. Simulations were run for three years in which year
52 2003 was spin-up and concentration results were analyzed for years 2004-2005. Since the
53 GEOS-4 re-analysis provides a reconstruction of the motion of the atmosphere through
54 actual time, the modeled concentrations should be comparable to those measured in
55 samples taken at specific times and places in the atmosphere, provided accurate fluxes are
56 incorporated. Kawa et al. (2004) showed that PCTM exhibits considerable skill in matching
57 synoptic and seasonal variation in CO₂ concentration at sites where continuous
58 measurements of CO₂ were available, and PCTM simulations have been widely used for
59 inversions and data assimilation of carbon cycle processes (Lokupitiya et al. 2008, Parazoo
60 et al. 2011, Hammerling et al. 2012). Our global modeling studies combined with increased
61 atmospheric monitoring will open the way for using higher resolution approaches, e.g.
62 mesoscale or Lagrangian models.

62

¹ <http://code916.gsfc.nasa.gov/Public/Modelling/pctm/pctm.html>

² <http://gmao.gsfc.nasa.gov/systems/geos4>

63 The observed concentrations were compared with simulated concentrations from a
 64 range of PCTM simulations driven by alternative source and sink estimates (Table 1). All
 65 PCTM simulations were driven by biomass burning emissions scaled to the GFED global
 66 inventory (van der Werf et al. 2003), anthropogenic fluxes from Kettle et al. (2002), and an
 67 atmospheric OH sink estimated using GEOS4 monthly mean temperature and zonal mean
 68 OH (Bian et al. 2007). For terrestrial and ocean fluxes, the PCTM simulations used the
 69 Kettle inventory or the new flux estimates described below.

70 **Table 1.** A compilation of the global sources and sinks used for PCTM simulations of
 71 atmospheric COS (units are 1.0×10^9 g of Sulfur).

Sources	Kettle et al., 2000	This Study
Direct COS Flux from Oceans	39	39
Indirect COS Flux as DMS from Oceans	81	81
Indirect COS Flux as CS ₂ from Oceans	156	156
Direct Anthropogenic Flux	64	64
Indirect Anthropogenic Flux from CS ₂	116	116
Indirect Anthropogenic Flux from DMS	0.5	0.5
Biomass Burning	11	136
Additional (photochemical) Ocean Flux		600
Sinks		
Destruction by OH Radical	-94	-101
Uptake by Canopy	-238	-738
Uptake by Soil	-130	-355
Net Total	-5	-2.5

72

73 Global Surface Fluxes

74 The gridded flux inventory of COS presented by Kettle et al. (2002) is the starting
 75 point for this modeling study (Table 1). Simulations with PCTM using these sources and
 76 sinks match the background concentration of COS fairly well, but as shown in Figure 1
 77 seasonal variation of COS at continental sites is too small. This is not surprising since
 78 Kesselmeier and co-workers have suggested a substantially larger uptake by leaves

79 (Sandoval-Soto et al. 2005) and soils (Van Diest and Kesselmeier 2008 and loc. cit.) based
80 on chamber studies. Protoschill-Krebs et al. (1996) identified that the biochemical
81 mechanism responsible for uptake of COS by leaves and soils is a hydrolysis reaction
82 catalyzed by the enzyme carbonic anhydrase leading to production of H₂S and CO₂.
83 However, this new information has not previously been used to construct a model for COS
84 exchange by plants and soil that could be run globally. We chose to use the carbon cycle
85 model SiB 3 (Baker et al. 2007, Baker et al. 2008) for this purpose in the present study.

86

87 **SiB 3 COS Leaf Uptake**

88 CO₂ and COS take the same pathway for diffusion from the atmosphere to the site of
89 reaction in leaves. COS is consumed inside leaf cells by the enzyme carbonic anhydrase
90 (CA) which is co-located in the chloroplasts of leaves with Rubisco - the enzyme that
91 consumes CO₂ in the first step of photosynthesis. The dynamic system of biochemical and
92 biophysical processes controlling the uptake of CO₂ by leaves is solved in SiB3 by a process
93 model based on Collatz et al. (1991). The corresponding conductance values for COS
94 calculated by SiB are adjusted for the difference in diffusivity (Stimler et al. 2010) of
95 H₂O: COS in the laminar boundary layer (1.56) and stomatal pore (1.94) (Figure 2). Liquid
96 phase and aerodynamic conductances to COS were assumed to be equal to that for CO₂. In
97 addition a rate expression for the reaction of COS with H₂O catalyzed by carbonic
98 anhydrase is needed (J_{COS}). Since the ambient concentration of COS is much lower than its
99 Michaelis-Menten half-saturation constant, we approximate this as a first order process:

$$100 \quad J_{\text{COS}} = [\text{COS}]_c * k * P \quad (1)$$

101 where $[\text{COS}]_c$ is the COS mole fraction in the chloroplast, P is the total pressure and k is a
102 first order rate constant ($\text{mol m}^{-2} \text{s}^{-1} \text{Pa}^{-1}$). We assume that the amount of CA activity is
103 proportional to the total amount of Rubisco, and responds to water stress and temperature
104 variation in parallel with Rubisco:

$$105 \quad k = 0.04 V_{\text{maxo}} * 2.1^{k_t} * \text{rstfac2} * \text{aparkk} \quad (2)$$

106 Where V_{maxo} , k_t , rstfac2 , and aparkk are constants from the SiB photosynthesis module (see
107 Collatz et al. 1991). Note, however, that CA activity is independent of light and CO₂
108 concentration, variables that strongly modulate the CO₂ uptake by Rubisco in vivo.

109 The flux of COS uptake by leaves can then be approximated as:

$$110 \quad J_{\text{leaf}} = [\text{COS}]_a * [1.94/g_{\text{sw}} + 1.56/g_{\text{bw}} + 1.0/g_i + 1.0/(k*P)]^{-1} \quad (3)$$

111 where $[\text{COS}]_a$ is the COS mixing ratio in the canopy air space and the terms in brackets
112 represent the series conductance of the leaf system for COS calculated from the respective
113 conductances to water vapor (Figure 2). The numerical coefficient of k was calibrated to
114 match observations of leaf exchange reported by Stimler et al. (2010). More physiological
115 studies are needed to calibrate this coefficient for a broader range of global vegetation
116 types, but we are confident that this parameterization captures the current understanding
117 of the mechanism of COS uptake by leaves.

118

119 **SiB-3 COS Soil Uptake**

120 The enzyme carbonic anhydrase also occurs in soil organisms (Seibt et al. 2006,
121 Wingate et al. 2008). Thus, COS that diffuses into the soil can also be hydrolyzed. The rate
122 is a function of the activity of CA the temperature of the soil and its porosity and water
123 content (Van Diest and Kesselmeier 2008). All of the above except the activity of CA are

124 physical properties of the soil that are simulated in SiB3. Although we lack direct
125 information on CA activity, it is likely to vary with the microbial biomass in the soil and
126 with temperature and water availability. Therefore, we have chosen to assume that the CA
127 activity is linked to the rate of heterotrophic respiration in the upper layers of soil (which is
128 simulated by SiB):

$$129 \quad J_{\text{soil}} = R_h * k_{\text{soil}} * f(w) \quad (4)$$

130 where R_h is the instantaneous rate of heterotrophic respiration, k_{soil} is an arbitrary scaling
131 factor, and $f(w)$ is a function to adjust for the difference in the soil moisture dependence of
132 COS uptake and R_h (Van Diest and Kesselmeier 2008). R_h is modeled as a function of soil
133 moisture and temperature, but is adjusted in SiB such that the seasonal total of CO2 release
134 in heterotrophic respiration is equal to the seasonal total of net primary production, (see
135 Baker et al. (2007) and Denning et al. (1996)). This empirical approach was able to
136 reproduce the responses of COS uptake to soil temperature and moisture observed in
137 chamber studies by van Diest and Kesselmeier (2008) and Seibt (unpublished). It is
138 recognized that this could be replaced by a more mechanistic approach in future work, but
139 at the moment there are very few studies of soil COS fluxes to parameterize a more detailed
140 model.

141

142 **Ecosystem Simulations**

143 Simulations were conducted with SiB-3.0-COS over a range of ecosystems using surface
144 meteorology derived from reanalysis (NCEP-2; Kalnay et al. 1996, Kanamitsu et al. 2002)
145 and vegetation dynamics and density derived from satellite observations (GIMMSg
146 normalized difference vegetation index; Brown et al. 2004, Tucker et al. 2005, Pinzon et al.

147 2006). Figure 3 shows typical diurnal courses of CO₂ and COS exchange for an Amazon
148 forest ecosystem near the end of the dry season. These simulations do not specify the COS
149 leaf fluxes as a fixed ratio to the CO₂ leaf fluxes – as has been done previously (Sandoval-
150 Soto et al. 2005, Campbell et al. 2008, Suntharalingam et al. 2008). Instead, these new flux
151 estimates are calculated by the mechanistic parameterization based on environmental
152 conditions, stomatal conductance and physiological stress as simulated by SiB.

153

154 **Results and Discussion**

155 **Revised ocean source**

156 SiB 3 was used to simulate fluxes of CO₂ and COS hourly at 1x1 degree grid, globally
157 for 2000-2005. However, as shown in Table 1, the total land sink was approximately 3-fold
158 larger in the SiB-based simulations than originally estimated by Kettle et al. (2002). Initial
159 simulations with this ocean source up-scaled according to the Kettle fluxes resulted in large
160 errors in the seasonal and latitudinal variation in atmospheric COS concentration (Figure
161 4). To reduce the error between steady-state COS simulations and observations, it was
162 necessary to make a corresponding adjustment in the modeled sources (Table 1). Thus, we
163 proposed a large ocean source, additional to the sources reported by Kettle et al. (2002).

164 Following Cutter et al. (2004), we added a photochemical source distributed
165 proportionally to solar radiation on the ocean. Monthly gridded marine insolation maps
166 were multiplied by a constant to close the COS budget. We then used a simple inversion
167 approach to optimize the latitudinal distribution of this ocean source in order to obtain a
168 better fit to the data while maintaining mass balance. Time-varying gridded fluxes of this
169 oceanic source COS were provided as a boundary condition for PCTM, which then predicted

170 the concentrations of COS at each of 14 NOAA atmospheric background sites. A linear
171 solver was then used to determine adjustments for the fluxes in each latitudinal band that
172 provided the best fit to the observed mean annual COS concentration. The resulting
173 distribution of this optimized ocean COS source is concentrated in the tropics (slightly
174 more than would be expected by solar insolation), with consequently lower intensities in
175 the higher latitudes of both hemispheres (Figure 4a). The main improvements to the
176 model versus observations are found at higher latitudes (Figure 4b). This latitudinal
177 distribution for a missing source is consistent with the results of a global analysis that was
178 based on an empirical model of terrestrial surface fluxes (Suntharalingam et al. 2008).

179

180 **Validation: seasonal cycle at GMD sites**

181 A reasonable fit for the COS concentrations was obtained at the background stations
182 (Figure 5) and the continental sites (Figure 1), and the new boundary conditions presented
183 here better approximate the observations than the prior Kettle boundary conditions. The
184 largest model-data mismatches are now found at MLO and NWR, sites not strongly
185 impacted by the terrestrial sink. The atmospheric simulations predict substantial
186 longitudinal gradients in concentration across large ocean basins and continental masses.
187 Measurement campaigns are currently underway that will empirically quantify these
188 gradients and test this prediction.

189

190 **Validation: vertical & spatial gradients**

191 The strong surface uptake simulated in the present study results in a strong draw-
192 down of the atmospheric boundary layer concentrations relative to the concentrations in

193 the free troposphere. There are many observations of these vertical gradients from recent
194 atmospheric sampling campaigns (Montzka et al. 2004, Blake et al. 2008, Campbell et al.
195 2008). Figure 6 shows data for a single vertical profile from the NASA-TC⁴ mission in the
196 Columbian Amazon in 2007 (Toon et al. 2010). At one point the plane dropped down into
197 the ABLE, where the COS concentration dropped abruptly by 50 ppt and CO₂ by 10 ppm.
198 These profiles are very similar to those simulated for the monthly mean profile at that grid
199 box in PCTM.

200 Figure 7 shows the mean vertical profile for the Mid-continent of North America
201 during the active growing season from the INTEX-NA mission in July and August of 2004
202 (Blake et al. 2008, Campbell et al. 2008). The enhanced uptake from the SiB model
203 provides an improved match for the observed INTEX-NA drawdown relative to the
204 simulations based on the much smaller sinks in the Kettle inventory. The simulations
205 based on the Kettle input show a surface enhancement rather than drawdown because the
206 anthropogenic fluxes are larger than the Kettle plant and soil fluxes in the Mid-continent
207 region. These preliminary tests provide validation of the new land flux used in the current
208 model, and indicate that a strong continental source is unlikely. We will pursue more
209 detailed point-by-point comparisons and improved COS flux parameterizations in the
210 future.

211

212 **Validation: Vertical-Latitudinal gradients in HIPPO**

213 While our top-down estimate of the ocean flux is concentrated in the tropics, there are
214 relatively few observations in tropical regions to confirm or refute the presence of such a
215 large emission. In a few samples collected in a recent airborne campaign, HIAPER Pole-to-

216 Pole Observations (HIPPO), enhanced COS concentrations were noted (Figure 8) over the
217 tropical Pacific ocean during the January 2009 deployment, providing some qualitative
218 support for the proposed ocean source (Wofsy et al. 2011)³. Such elevated concentrations
219 were not widespread, and they did not appear in HIPPO deployments during other seasons,
220 suggesting the possibility that this source might be heterogeneously distributed in time and
221 space within the tropics. Additional observations in the tropics will clearly be needed to
222 constrain the magnitude of COS fluxes in this region.

223

224 **Outlook:**

225 **Using differential patterns in COS and CO₂ drawdown to diagnose carbon cycle** 226 **processes**

227 We designed a simulation experiment to examine if differential responses of
228 photosynthesis and respiration could be seen from hypothetical atmospheric
229 measurements of COS and CO₂. We conducted two global simulations each with a different
230 implementation of soil hydrology and water stress. The original SiB version was known
231 from comparisons with ecosystem scale measurements at an eddy correlation tower in the
232 Eastern Amazon near Santaram to over-estimate drought stress. In the original simulation,
233 the canopy developed severe water stress near the end of the dry season, yet this was not
234 seen in the eddy correlation studies conducted in the forest. To correct this problem, the
235 soil was made deeper and root-mediated redistribution of soil water was implemented in a

235

³ <ftp://cdiac.ornl.gov/pub/HIPPO/>

236 new version of the SiB model (Baker et al. 2008), following Kleidon and Heimann (2000).
237 This modification reduced the simulated inhibition of photosynthesis and enhanced COS
238 uptake by eliminating soil water stress. The two different model implementations were
239 run globally, including atmospheric transport simulated by PCTM. Figure 9 shows plots of
240 the difference in the simulated mid-boundary layer concentration draw-down for CO₂ and
241 COS over South America. The model with the improved hydrology showed stronger draw-
242 down of both COS and CO₂ in the ABL over Eastern Amazon, which was consistent with the
243 difference seen in site level simulations. In this region, maps of the fluxes coincided with
244 the simulated atmospheric tracer anomalies. Examination of the simulated fluxes showed
245 that photosynthesis and COS uptake were enhanced by the improved soil hydrology.
246 However, respiration was not greatly effected, and consequently there was an enhanced
247 draw-down of CO₂ in addition to COS.

248 The changed soil moisture parameterization also had strong effects on the
249 concentrations of COS and CO₂ over other areas of South America, but unlike the Eastern
250 Amazon, the two species did not change in tandem. In particular, note the enhanced COS
251 draw-down to the south of the Amazon basin that was *not* accompanied by an enhanced
252 CO₂ draw-down. Inspection of the simulated fluxes in that region indicated that
253 photosynthesis was indeed stimulated in this area, but in contrast to the forest ecosystem
254 to the north, respiration was also stimulated, neutralizing changes in net ecosystem CO₂
255 exchange. This region is a grassland ecosystem with shallower soils and more roots near
256 the surface. Apparently the new hydrology resulted in more soil moisture in surface layers,
257 that stimulated both photosynthesis and respiration. Thus there was no net effect on CO₂
258 flux. Another area in the Western Amazon shows decreased COS draw-down with little or

259 no CO₂ effect. The change in hydrology depressed both photosynthesis and respiration in
260 this region. These simulations provide interesting examples of differential responses of
261 photosynthesis and respiration that have clearly interpretable manifestations in the
262 comparative drawdown of CO₂ and COS. Clearly, COS data could provide process level
263 insights additional to those we could distinguish from only studying the CO₂ concentration.

264 In summary, we demonstrated using a simulation experiment that COS data could
265 provide additional information on the separate responses of photosynthesis and
266 respiration to environmental forcing. The simulations presented here indicate that
267 measurement of COS could provide improved constraints on 4-D data assimilation of
268 carbon cycle processes.

269

270 **Acknowledgements**

271 We gratefully acknowledge Mohammad Abu-Naser for help preparing figures. SAM
272 acknowledges the support of the Atmospheric Composition and Climate Program and the
273 Carbon Cycle Program of NOAA's Climate Program Office for making COS measurements
274 from surface sites and aircraft.

References

- Baker, I. T., A. S. Denning, L. Prihodko, K. Schaefer, J. A. Berry, G. J. Collatz, N. S. Suits, R. Stockli, A. Philpott, and O. Leonard. 2007. Global Net Ecosystem Exchange (NEE) of CO₂. Oak Ridge National Laboratory Distributed Active Archive Center.
- Baker, I. T., L. Prihodko, A. S. Denning, M. Goulden, S. Miller, and H. R. da Rocha. 2008. Seasonal drought stress in the Amazon: Reconciling models and observations. *Journal of Geophysical Research-Biogeosciences* **113**.
- Barkley, M. P., P. I. Palmer, C. D. Boone, P. F. Bernath, and P. Suntharalingam. 2008. Global distributions of carbonyl sulfide in the upper troposphere and stratosphere. *Geophysical Research Letters* **35**.
- Bian, H., M. Chin, S. R. Kawa, B. Duncan, A. Arellano, and P. Kasibhatla. 2007. Sensitivity of global CO simulations to uncertainties in biomass burning sources. *Journal of Geophysical Research-Atmospheres* **112**.
- Blake, N. J., J. E. Campbell, S. A. Vay, H. E. Fuelberg, L. G. Huey, G. Sachse, S. Meinardi, A. Beyersdorf, A. Baker, B. Barletta, J. Midyett, L. Doezema, M. Kamboures, J. McAdams, B. Novak, F. S. Rowland, and D. R. Blake. 2008. Carbonyl sulfide (OCS): Large-scale distributions over North America during INTEX-NA and relationship to CO₂. *Journal of Geophysical Research-Atmospheres* **113**.
- Blonquist, J. M., S. A. Montzka, J. W. Munger, D. Yakir, A. R. Desai, D. Dragoni, T. J. Griffis, R. K. Monson, R. L. Scott, and D. R. Bowling. 2011. The potential of carbonyl sulfide as a proxy for gross primary production at flux tower sites. *Journal of Geophysical Research-Biogeosciences* **116**.
- Brown, M. E., J. Pinzon, and C. J. Tucker. 2004. New Vegetation Index Dataset Available to Monitor Global Change. *EOS Transactions* **85**:565.
- Campbell, J. E., G. R. Carmichael, T. Chai, M. Mena-Carrasco, Y. Tang, D. R. Blake, N. J. Blake, S. A. Vay, G. J. Collatz, I. Baker, J. A. Berry, S. A. Montzka, C. Sweeney, J. L. Schnoor, and C. O. Stanier. 2008. Photosynthetic Control of Atmospheric Carbonyl Sulfide During the Growing Season. *Science* **322**:1085-1088.
- Collatz, G. J., J. T. Ball, C. Grivet, and J. A. Berry. 1991. Physiological and Environmental-Regulation of Stomatal Conductance, Photosynthesis and Transpiration - a Model That Includes a Laminar Boundary-Layer. *Agricultural and Forest Meteorology* **54**:107-136.
- Cutter, G. A., L. S. Cutter, and K. C. Filippino. 2004. Sources and cycling of carbonyl sulfide in the Sargasso Sea. *Limnology and Oceanography* **49**:555-565.
- Denning, A. S., G. J. Collatz, C. G. Zhang, D. A. Randall, J. A. Berry, P. J. Sellers, G. D. Colello, and D. A. Dazlich. 1996. Simulations of terrestrial carbon metabolism and atmospheric CO₂ in a general circulation model .1. Surface carbon fluxes. *Tellus Series B-Chemical and Physical Meteorology* **48**:521-542.
- Hammerling, D. M., A. M. Michalak, C. O'Dell, and S. R. Kawa. 2012. Global CO₂ distributions over land from the Greenhouse Gases Observing Satellite (GOSAT). *Geophysical Research Letters* **39**.
- Kalnay, E., M. Kanamitsu, R. Kistler, W. Collins, D. Deaven, L. Gandin, M. Iredell, S. Saha, G. White, J. Woollen, Y. Zhu, M. Chelliah, W. Ebisuzaki, W. Higgins, J. Janowiak, K. C. Mo, C. Ropelewski, J. Wang, A. Leetmaa, R. Reynolds, R. Jenne, and D. Joseph. 1996. The

- NCEP/NCAR 40-year reanalysis project. *Bulletin of the American Meteorological Society* **77**:437-471.
- Kanamitsu, M., W. Ebisuzaki, J. Woollen, S. K. Yang, J. J. Hnilo, M. Fiorino, and G. L. Potter. 2002. NCEP-DOE AMIP-II Reanalysis (R-2). *Bulletin of the American Meteorological Society* **83**:1631-1643.
- Kawa, S. R., D. J. Erickson, S. Pawson, and Z. Zhu. 2004. Global CO₂ transport simulations using meteorological data from the NASA data assimilation system. *Journal of Geophysical Research-Atmospheres* **109**.
- Kettle, A. J., U. Kuhn, M. von Hobe, J. Kesselmeier, and M. O. Andreae. 2002. Global budget of atmospheric carbonyl sulfide: Temporal and spatial variations of the dominant sources and sinks. *Journal of Geophysical Research-Atmospheres* **107**.
- Kleidon, A. and M. Heimann. 2000. Assessing the role of deep rooted vegetation in the climate system with model simulations: mechanism, comparison to observations and implications for Amazonian deforestation. *Climate Dynamics* **16**:183-199.
- Lokupitiya, R. S., D. Zupanski, A. S. Denning, S. R. Kawa, K. R. Gurney, and M. Zupanski. 2008. Estimation of global CO₂ fluxes at regional scale using the maximum likelihood ensemble filter. *Journal of Geophysical Research-Atmospheres* **113**.
- Montzka, S. A., M. Aydin, M. Battle, J. H. Butler, E. S. Saltzman, B. D. Hall, A. D. Clarke, D. Mondeel, and J. W. Elkins. 2004. A 350-year atmospheric history for carbonyl sulfide inferred from Antarctic firn air and air trapped in ice. *Journal of Geophysical Research-Atmospheres* **109**.
- Montzka, S. A., P. Calvert, B. D. Hall, J. W. Elkins, T. J. Conway, P. P. Tans, and C. Sweeney. 2007. On the global distribution, seasonality, and budget of atmospheric carbonyl sulfide (COS) and some similarities to CO₂. *Journal of Geophysical Research-Atmospheres* **112**.
- Parazoo, N. C., A. S. Denning, J. A. Berry, A. Wolf, D. A. Randall, S. R. Kawa, O. Pauluis, and S. C. Doney. 2011. Moist synoptic transport of CO₂ along the mid-latitude storm track. *Geophysical Research Letters* **38**.
- Pinzon, J., M. E. Brown, and C. J. Tucker. 2006. Satellite Time Series Correction of Orbital Drift Artifacts Using Empirical Mode Decomposition. *in* N. Huang, editor. *Applications of Empirical Mode Decomposition, Part II*.
- Protoschill-Krebs, G., C. Wilhelm, and J. Kesselmeier. 1996. Consumption of carbonyl sulphide (COS) by higher plant carbonic anhydrase (CA). *Atmospheric Environment* **30**:3151-3156.
- Sandoval-Soto, L., M. Stanimirov, M. von Hobe, V. Schmitt, J. Valdes, A. Wild, and J. Kesselmeier. 2005. Global uptake of carbonyl sulfide (COS) by terrestrial vegetation: Estimates corrected by deposition velocities normalized to the uptake of carbon dioxide (CO₂). *Biogeosciences* **2**:125-132.
- Seibt, U., L. Wingate, J. Lloyd, and J. A. Berry. 2006. Diurnally variable delta(18)O signatures of soil CO₂ fluxes indicate carbonic anhydrase activity in a forest soil. *Journal of Geophysical Research-Biogeosciences* **111**.
- Stimler, K., S. A. Montzka, J. A. Berry, Y. Rudich, and D. Yakir. 2010. Relationships between carbonyl sulfide (COS) and CO₂ during leaf gas exchange. *New Phytologist* **186**:869-878.

- Suntharalingam, P., A. J. Kettle, S. M. Montzka, and D. J. Jacob. 2008. Global 3-D model analysis of the seasonal cycle of atmospheric carbonyl sulfide: Implications for terrestrial vegetation uptake. *Geophysical Research Letters* **35**.
- Toon, O. B., D. O. Starr, E. J. Jensen, P. A. Newman, S. Platnick, M. R. Schoeberl, P. O. Wennberg, S. C. Wofsy, M. J. Kurylo, H. Maring, K. W. Jucks, M. S. Craig, M. F. Vasques, L. Pfister, K. H. Rosenlof, H. B. Selkirk, P. R. Colarco, S. R. Kawa, G. G. Mace, P. Minnis, and K. E. Pickering. 2010. Planning, implementation, and first results of the Tropical Composition, Cloud and Climate Coupling Experiment (TC4). *Journal of Geophysical Research-Atmospheres* **115**.
- Tucker, C. J., J. E. Pinzon, M. E. Brown, D. A. Slayback, E. W. Pak, R. Mahoney, E. F. Vermote, and N. El Saleous. 2005. An extended AVHRR 8-km NDVI dataset compatible with MODIS and SPOT vegetation NDVI data. *International Journal of Remote Sensing* **26**:4485-4498.
- van der Werf, G. R., J. T. Randerson, G. J. Collatz, and L. Giglio. 2003. Carbon emissions from fires in tropical and subtropical ecosystems. *Global Change Biology* **9**:547-562.
- Van Diest, H. and J. Kesselmeier. 2008. Soil atmosphere exchange of carbonyl sulfide (COS) regulated by diffusivity depending on water-filled pore space. *Biogeosciences* **5**:475-483.
- Wingate, L., U. Seibt, K. Maseyk, J. Ogee, P. Almeida, D. Yakir, J. S. Pereira, and M. Mencuccini. 2008. Evaporation and carbonic anhydrase activity recorded in oxygen isotope signatures of net CO₂ fluxes from a Mediterranean soil. *Global Change Biology* **14**:2178-2193.
- Wofsy, S. C., H. S. Team, C. M. Team, and S. Team. 2011. HIAPER Pole-to-Pole Observations (HIPPO): fine-grained, global-scale measurements of climatically important atmospheric gases and aerosols. *Philosophical Transactions of the Royal Society a-Mathematical Physical and Engineering Sciences* **369**:2073-2086.
- Wohlfahrt, G., F. Brilli, L. Hortnagl, X. B. Xu, H. Bingemer, A. Hansel, and F. Loreto. 2012. Carbonyl sulfide (COS) as a tracer for canopy photosynthesis, transpiration and stomatal conductance: potential and limitations. *Plant Cell and Environment* **35**:657-667.

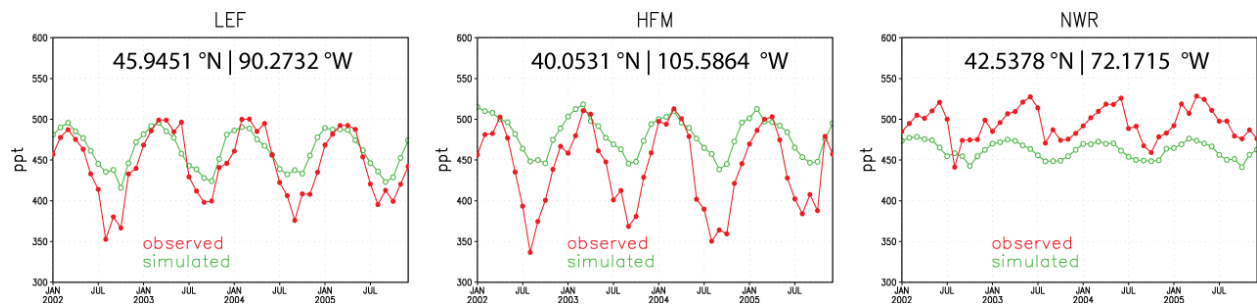


Figure 1. Simulated and observed COS monthly mean concentrations at the WLEF tower in Wisconsin, Harvard Forest, and Niwot Ridge using the sources and sinks given by Kettle et al., (2002). Data from NOAA-ESRL global monitoring network (Montzka et al., 2007).

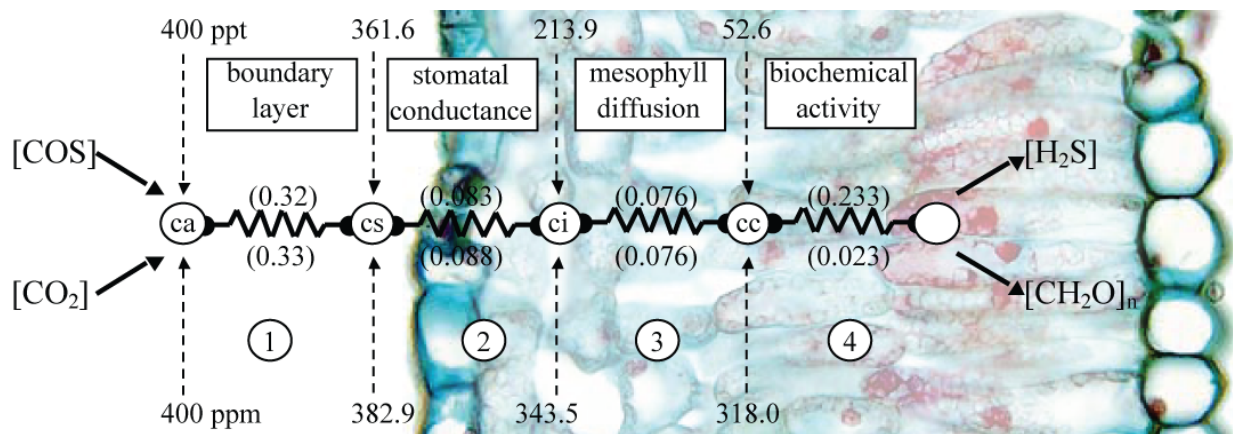


Figure 2. Resistance analog model of CO_2 and COS uptake. Numbers in parentheses are conductance values ($\text{mol m}^{-2} \text{s}^{-1}$) corresponding to the numbered key: (1) Boundary layer conductance, g_b . (2) Stomatal conductance, g_s . (3) Mesophyll conductance, g_i . (4) Biochemical rate constant used approximate photosynthetic CO_2 uptake by Rubisco or the reaction of COS with carbonic anhydrase as a linear function of c_c . In this case COS uptake is $12.6 \text{ } \mu\text{mol m}^{-2} \text{s}^{-1}$ and that of CO_2 is $5.6 \text{ } \mu\text{mol m}^{-2} \text{s}^{-1}$.

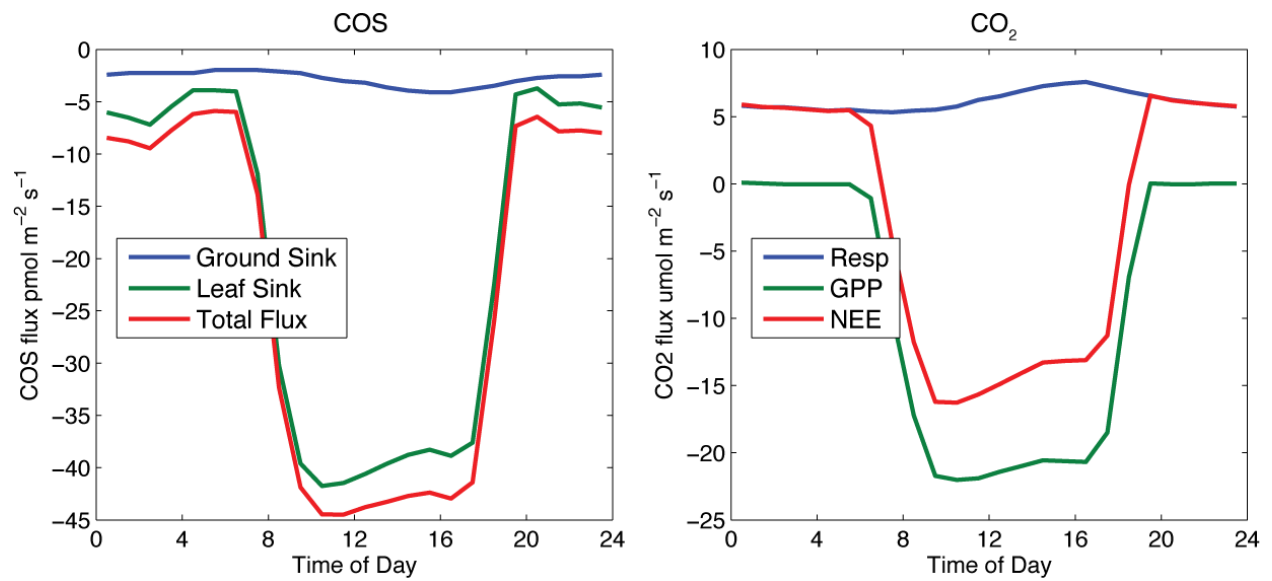


Figure 3. Diel variation in CO₂ and COS exchange simulated at the Km 83 site near Santarem Brazil. Note that daytime GPP and leaf COS uptake are parallel. COS uptake by the soil is not correlated with GPP and some leaf and soil uptake continues at night owing to incomplete stomatal closure.

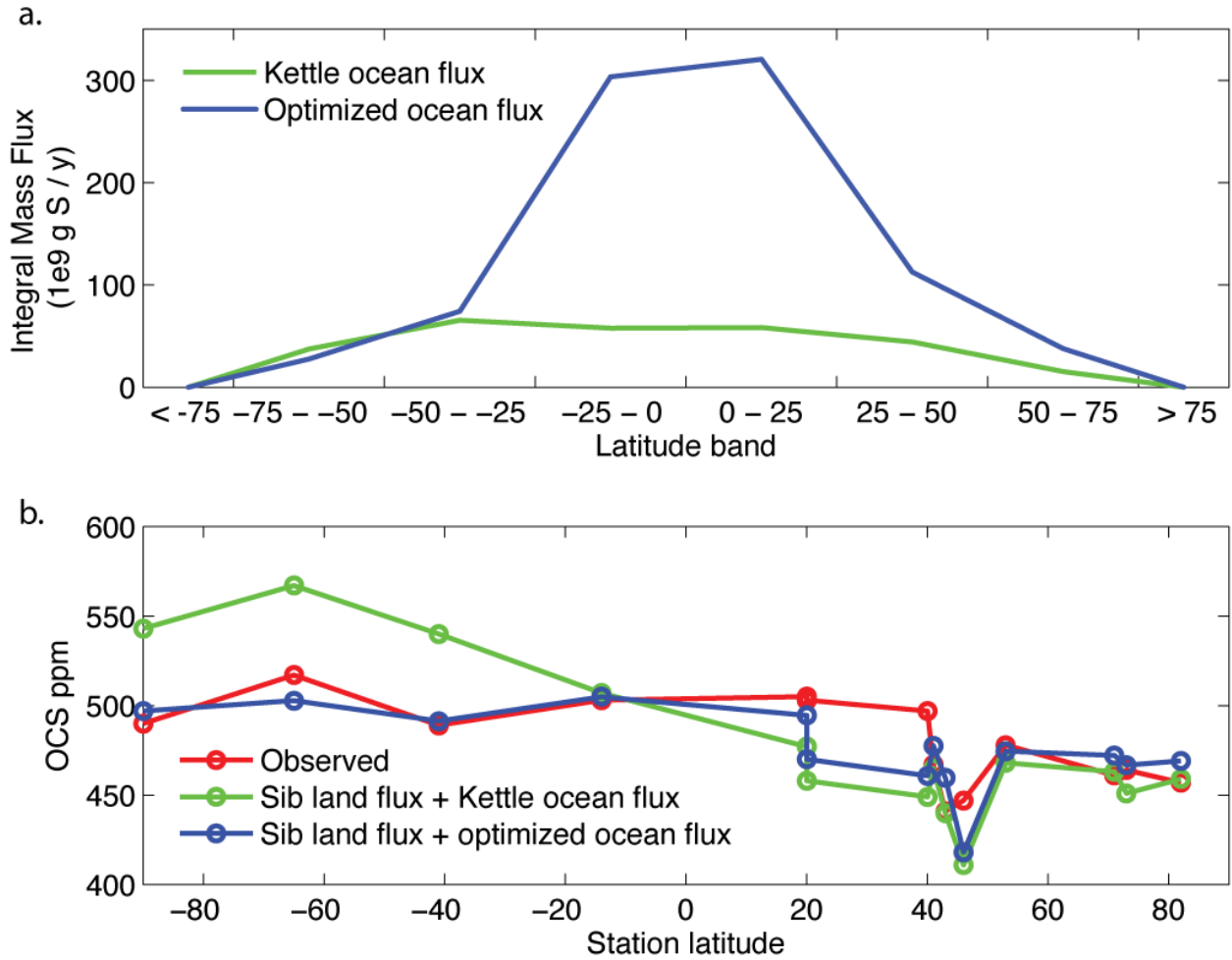


Figure 4. The original and optimized latitudinal distribution of the ocean source used in this study. a: Mass fluxes for each latitude band. b: Comparison with surface station annual mean observations. Sites are ALT, SUM, BRW, MHD, LEF, HFM, THD, NWR, MLO, KUM, SMO, CGO, PSA, SPO. Data from NOAA-ESRL global monitoring network (Montzka et al., 2007).

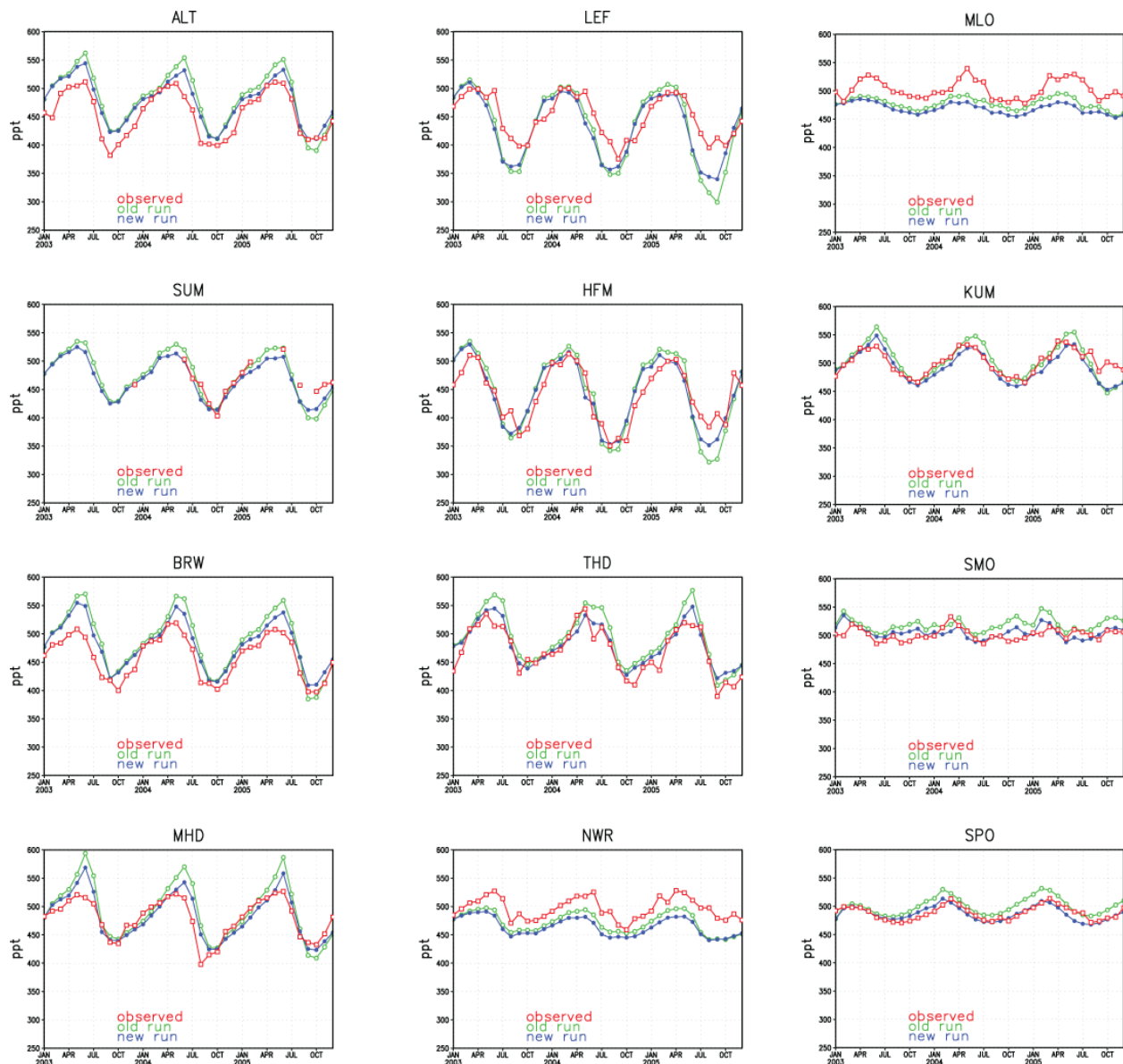


Figure 5. Seasonal variation in simulated COS concentration compared to the corresponding monthly mean observations at the NOAA background atmosphere sampling stations. Data from NOAA-ESRL global monitoring network (Montzka et al., 2007).

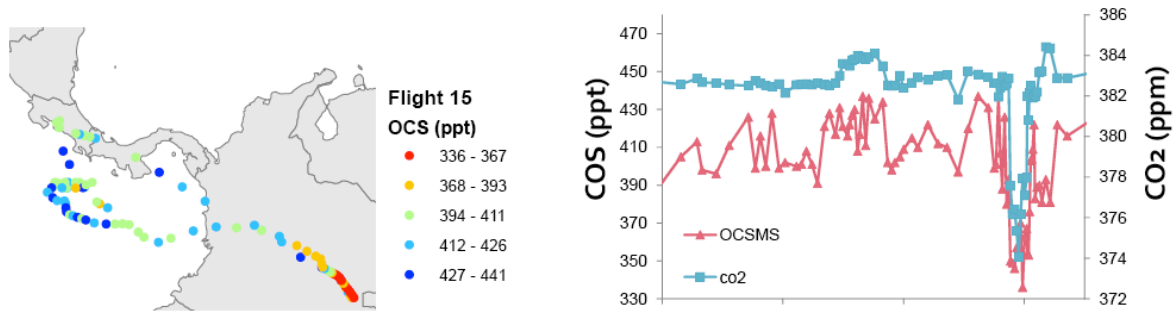


Figure 6. CO₂ and COS concentration measured in a flight of the TC4 campaign into the Columbian Amazon. Most of the flight was in the free troposphere except the portion with low CO₂ and COS ratios. Data from N. Blake.

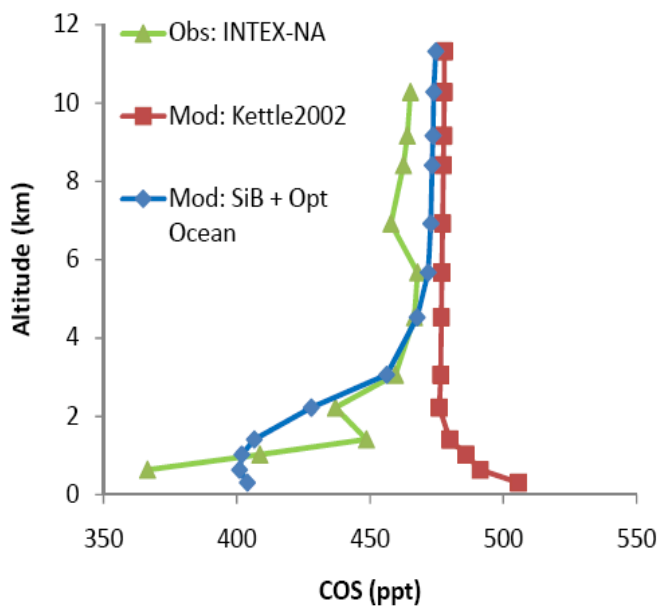


Figure 7. The monthly mean profile simulated by PCTM over Illinois and Indiana in July-August 2004 compared to the mean of flask samples taken by the INTEX- NA campaign. Data from Blake et al., (2008).

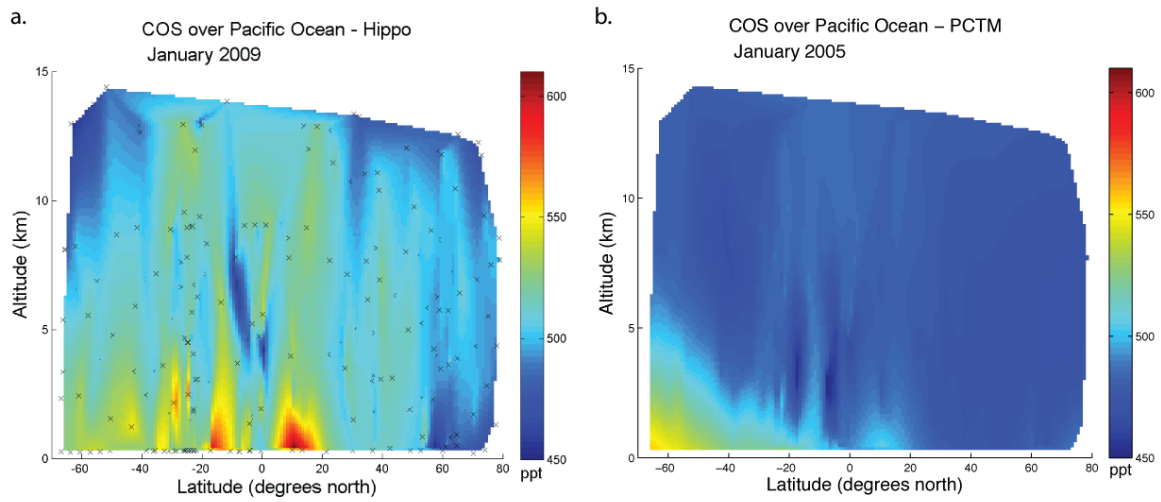
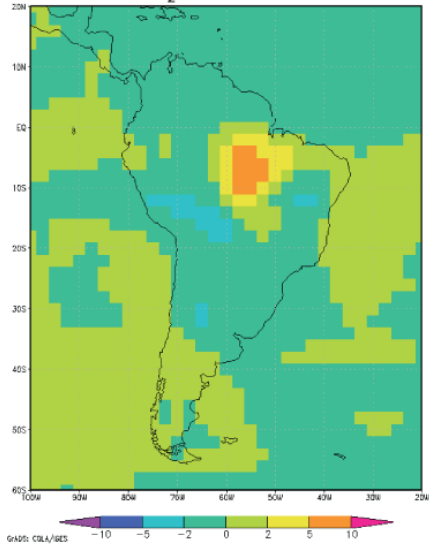
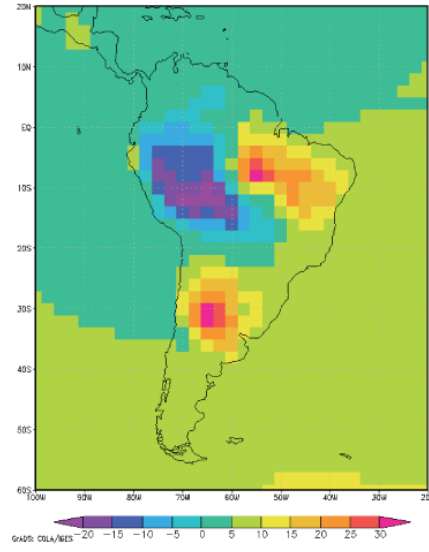


Figure 8: Comparison of COS latitude x altitude slice observed in HIPPO (a) with simulation in this study (b). The comparison is to evaluate the evidence for a large oceanic source proposed in this study; see text for discussion.

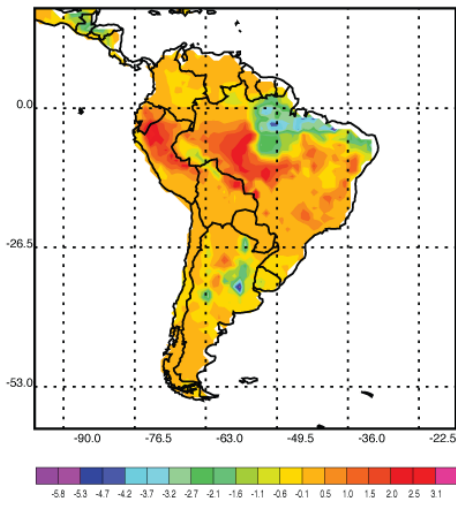
a. ΔCO_2 in ABL (ppm)



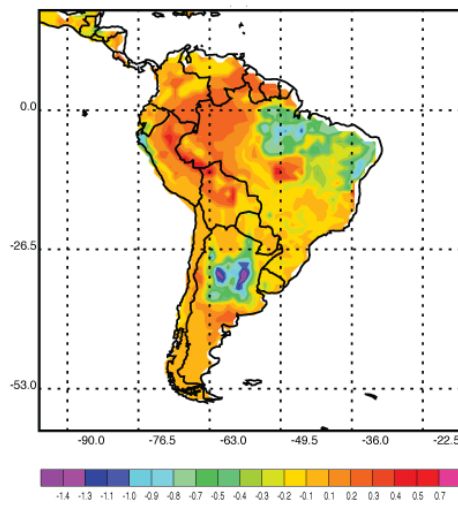
b. ΔCOS in ABL (ppt)



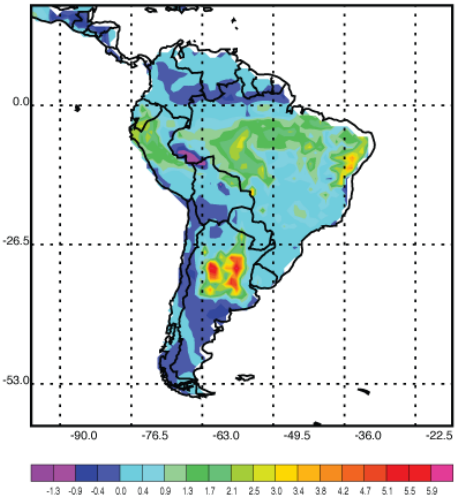
c. ΔNEE ($\text{umol}/\text{m}^2/\text{s}$)



d. $\Delta\text{COS flux}$ ($\text{umol}/\text{m}^2/\text{s} \times 10^{-5}$)



e. $\Delta\text{Respiration}$ ($\text{umol}/\text{m}^2/\text{s}$)



f. ΔGPP ($\text{umol}/\text{m}^2/\text{s}$)

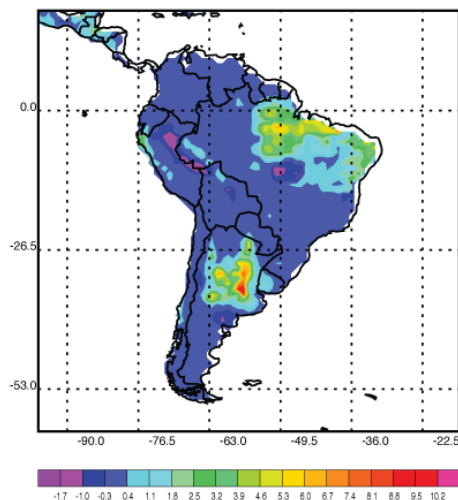


Figure 9. Maps illustrating the use of COS as a diagnostic between different land surface model soil hydrology implementations. Maps show the difference in ABL concentration (a-b) and surface fluxes (c-f) for CO₂ and COS for different parameterizations (new-old) over South America in January 2005. Positive values in panels a and b indicate increased drawdown indicative of increased net uptake in the new parameterization; negative values in panels c-f indicate increased flux. An area of enhanced CO₂ draw-down (5-10 ppm) in the ABL is seen over the Eastern Amazon, with corresponding enhanced COS draw-down (20-40ppt) over the same area. Another area of COS draw-down is seen over an area south of the Amazon, but with no corresponding area of enhanced CO₂ draw-down. See the text for interpretation.